Polymer Chemistry

Accepted Manuscript

ROYAL SOCIETY OF CHEMISTRY

www.rsc.org/polymers

Enhanced visible radiation photopolymerization of dimethacrylates with the three component thioxanthone (CPTXO) - amine - iodonium salt system.

Wayne D. Cook* and Fei Chen

Department of Materials Engineering, Wellington Road,
Monash University, Victoria 3800, Australia

* To whom correspondence should be addressed.

*Mailing address: Prof Wayne D. Cook
Rm 115/Bldg 69
Department of Materials Engineering
Wellington Road, Monash University,
Victoria 3001, Australia

E-mail: Wayne.Cook@ monash.edu
Telephone: +613 9905 4926
Fax: +613 9905 4940

Abstract

Photo-DSC and UV-visible spectroscopy were used to study the photo-curing kinetics and mechanism of the photopolymerization of dimethacrylates using three-component initiation systems consisting of 1-chloro-4-propoxy-9H-thioxanthen-9-one (CPXTO), diphenyl iodonium hexafluorophosphate (Ph_2IPF_6), and the aromatic N,N,3,5-tetramethyl aniline (TMA) or the aromatic-like N,N-dimethylbenzylamine or aliphatic triethylamine. The effect of monomers with different backbone flexibilities on the curing kinetics were also investigated, using aliphatic triethylene glycol dimethacrylate (TEGDMA), aliphatic nona-ethylene glycol dimethacrylate and aromatic diethoxylated bisphenol-A dimethacrylate. Photo-DSC cure kinetics studies showed that the fastest polymerization occurred when all three components were present for CPTXO/amine/Ph_2IPF_6 systems, and the maximum polymerization rate followed the trend: CPTXO/amine/Ph_2IPF_6 >> CPTXO/Ph_2IPF_6 ≥ CPTXO/amine, irrespective of the monomer or amine used. UV-visible spectroscopy studies revealed that for the TEGDMA/CPTXO/TMA, TEGDMA/CPTXO/Ph_2IPF_6, and TEGDMA/CPTXO/TMA/Ph_2IPF_6 systems, the CPTXO was rapidly photobleached at its absorption maximum (near 385nm) during the photo-DSC timescale with photobleaching rates which followed the trend: CPTXO/TMA >> CPTXO/Ph_2IPF_6 ≈ CPTXO/TMA/Ph_2IPF_6. At the same time, a new absorption at 500nm appeared for the systems containing CPTXO and Ph_2IPF_6, and the rate of this photodarkening behavior was greater for the CPTXO/Ph_2IPF_6 system compared with CPTXO/TMA/Ph_2IPF_6, - no photodarkening at 500nm was found for the CPTXO/TMA system. Based on the curing kinetics, photobleaching studies and the thermodynamic feasibility it is proposed that for the three-component CPTXO/amine/Ph_2IPF_6 system, the reaction involves two main pathways. The first is the irreversible oxidation of the excited CPTXO molecule by Ph_2IPF_6 with the formation of a thioxanthone radical cation and a phenyl radical by an electron-transfer mechanism, followed

by H-transfer between a thioxanthone radical cation and amine (or monomer) to form an aminoalkyl radical and to also regenerate CPTXO. The second pathway involves the reduction of the excited CPTXO molecule by the amine to form ketyl and aminoalkyl radicals, followed by the irreversible oxidation of the amine and the ketyl radicals by the iodonium salt, to form an initiating radical and also to regenerate CPTXO. Due to the non-reversible oxidation of the CPTXO and amine radicals by the iodonium salt (which prevents the back-electron transfer of amine to the excited CPTXO), due to the CPTXO regeneration reactions and due to the removal of the potentially terminating CPTXO radical, the efficiency of the CPTXO/TMA/Ph_2IPF_6 photoinitiating system is dramatically enhanced.

Keywords: photopolymerization, three-component photoinitiator system, photo-DSC, kinetics, photobleaching, dimethacrylate

Introduction

Photopolymerization is used in many important applications, including composite production, prototyping, coating, adhesives, inks, and electronics [1-4]. Although UV radiation was the most common up till the 1980s, visible light initiated photopolymerization has become increasingly popular due to reduced cost and safety, particularly in biological applications such as dental restorations [5], orthopedics [6], and polymer scaffolds for tissue engineering [7]. In addition, for thick films, a higher conversion of monomer can be produced at greater depths with visible radiation due to the greater penetration range of longer wavelength light [8]. In some cases this effect is enhanced if the photoinitiator is photolysed into a colorless product (termed "photobleaching") because this enables further light penetration in thick systems [9].

Many visible light photoinitiation systems employ two components to increase the photoinitiation rate and also enhance the spectral sensitivity of the system[10]. For example, many common free radical photoinitiator systems [11] use a light absorbing ketone photosensitizer (e.g. the aliphatic camphorquinone, CQ [12] or an aromatic thioxanthone [13] as a photo-oxidizer and a reducer such as an amine or silane [14] - here the active centers are produced via electron transfer followed by proton transfer from the electron donor to the excited photosensitizer. Similarly, several cationic initiator systems employ a light absorbing reducer (e.g. an aromatic ketone [15] or a quinoxaline [16]) and an onium cation as an oxidizer [11] coupled with a non-nucleophilic anion, so that a superacid can be produced to initiate polymerization. Some groups have also been studying three-component photo-initiator systems [6, 11, 17-45], which contain a photosensitizer, an electron donor, and a third component, which is often an onium salt. Three component initiator systems have several advantages over the corresponding two-component initiator systems. These include enhanced polymerization rates at lower light intensities [18, 41], greater flexibility in selection of the

components[41] and the ability to initiate free-radical and cationic photopolymerizations simultaneously [46, 47].

However, in contrast to the two component redox photoinitiators, the three component systems are not well understood, and a number of different mechanisms using an onium salt have been proposed in the literature [11, 17-19, 22, 23, 29-33, 39, 41, 48] which can be loosely grouped into two general classes. The first category applies to parallel systems where two of the three components are involved in one initiating process while a second pair of the three components react via an independent process to form other initiating species [11, 19, 30, 39]. The second category applies to sequential reactions in which two of the three components first react with one another and the third component then reacts with the products of the first reaction [17, 18, 22, 23, 29, 31-33, 41].

As an example of parallel initiation, Padon and Scranton [19] studied a three-component system containing Eosin Y, *N*-methyldiethanolamine, and diphenyliodonium chloride. Based on the photo-DSC kinetics studies and laser-induced fluorescence experiments, it was concluded that there are simultaneous (parallel) reactions between the eosin and iodonium and between the eosin and amine. The three-component system consisting of a thioxanthene ketone (however not a thioxanthenone), N-phenylglycine and diphenyliodonium tetrafluoroborate is an example of the sequential mechanism. Here, Harada et al. [22] used electron spin resonance to show that the photoexcited thioxanthene reacts with the amine to form an amine radical cation and a thioxanthene carbonyl radical anion. The latter in turn reacts with the iodonium salt to produce an active phenyl radical and regenerate the thioxanthene ketone while the amine cation-radical donates a proton to the iodonium anion to form an active phenylaminomethyl radical.

In most of the mechanisms proposed, the photosensitizer is either oxidized or reduced during the photoinitiation and so changes in UV-visible absorption spectrum should be

observed. Recently, we used UV-vis spectroscopy in conjunction with photocalorimetry to investigate the photoinitiation mechanisms involved in the CQ/amine/iodonium three component initiating system[41], and these studies suggested that a sequential photoinitiation mechanism was involved, but there do not appear to have been any related studies of the thioxanthone bleaching and very limited work on the influence of each component (thioxanthone, amine and iodonium initiator) on the rate of photopolymerization of methacrylates and so the exact mechanisms of photoinitiation are unclear. In the present study, we have used the photo-DSC and steady-state UV-visible spectroscopy to investigate the photopolymerization kinetics and spectroscopy for the three-component system containing 1-chloro-4-propoxy-9H-thioxanthen-9-one as a light-absorbing molecule, various amines as the electron donor, and diphenyl iodonium hexafluorophosphate as a third component. The generality of the photoinitiation efficiency of these systems was studied by performing photopolymerization studies for three different monomers with varying backbone flexibilities and aromaticity.

Experimental

2.1. Materials

Triethylene glycol dimethacrylate (TEGDMA, Aldrich), which polymerizes to a rigid glass, was used as the principal monomer under investigation. Diethoxylated bisphenol-A dimethacrylate (DEBPADM, Sartomer) was used as an alternative glass-forming monomer because unlike TEGDMA it is an aromatic dimethacrylate. The molecular weight of the DEBPADM was determined to be 470 g/mol by titration of the methacrylate groups, which compares well with the theoretical value of 452 g/mol [49]. Nona-ethylene glycol dimethacrylate (NEGDMA, supplied by Aldrich as polyethylene glycol dimethacrylate with M_n ~550 g/mol) was also used for comparative purposes because this monomer polymerizes

into an elastomer - it should be noted that it is likely that the product contains a distribution of oligoethylene oxide units with an average of nine, as has been reported for a similar product [50].

The photosensitizer used was 0.20 wt% 1-chloro-4-propoxy-9H-thioxanthen-9-one (CPXTO, Aldrich). Either the aromatic tertiary amine, N,N,3,5-tetramethyl aniline (TMA, Aldrich) or the semi-aromatic tertiary amine, N,N-dimethylbenzylamine (DMBA, Aldrich) or the aliphatic tertiary amine, triethylamine (TEA, MERCK), was used as an electron donor at a concentration of 0.30 wt% in the monomer. The onium oxidant was diphenyl iodonium hexafluorophosphate (Ph_2IPF_6, Aldrich) used at a concentration of 1.00 wt% - this is a commonly used as photo cationic initiator[1] and has the advantage over iodonium halides of being more soluble in the monomer.

Although CPTXO has a maximum absorption at 390 nm, its molar absorptivity is so high that irradiation at this wavelength can cause problems with attenuation through the sample depth[51, 52]. Since the absorption tail of CPTXO extends into 430 nm, the monomer and initiator systems were photolysed using 415 nm radiation which avoided these self-absorption problems. The concentrations of the CPTXO and Ph_2IPF_6 were chosen based on previous work[51, 52] which showed that the attenuation of the radiation through the depth of the DSC sample was minimal and that the rate of polymerization were sufficiently high to be readily measurable by photo-DSC. All chemicals were used as received and their structures are shown in Scheme 1.

2.2. Photo-differential scanning calorimetry

Isothermal photopolymerization studies were performed in a Perkin-Elmer DSC-7 equipped with an Intracooler. The instrument was modified [53] to allow the irradiation of both the sample and reference DSC pans, minimizing the thermal imbalance created by the

radiation source. A poly(methyl methacrylate) (PMMA) block, with holes located directly above the DSC pan holders, was used in place of the standard DSC cover. Photopolymerization was performed using 415nm (390–440 nm, as measured with an Ocean Optics USA USB2000 fibre optic spectroradiometer) from a Polilight PL400 (Rofin, Australia) which has selectable wavelength regions defined by band-pass filters. The radiation was directed into a bifurcated glass fibre optic light guide (7mm diameter entry window, 5mm diameter exit windows), the legs of which were fitted into the holes in the PMMA block. Fine aluminium rings were placed on the ledge in each sample pan holder and two 0.05mm thick poly(ethylene terephthalate) (PET) covers (6mm diameter) with two vent holes were used to cover the DSC pan holders to prevent an unstable baseline and to minimize sample evaporation during the experiment [54]. Any remaining thermal imbalance in heat from the lamp onto the two pans was further corrected by repeating the illumination (sometimes several times to ensure no polymerization continued) of the "fully-cured" and reference in a second isothermal DSC run and subtracting the data from the first run – subsequent polymerization was not observed during the repeated illumination. All samples were photocured at 50 °C under a N_2 atmosphere at a flow rate of 20 mL min^{-1}. The samples were maintained under N_2 for a minimum of 5 min to exclude oxygen from the resin. To obtain stability of the radiation intensity, the light source was activated 60s before commencement of irradiation by use of a shutter in front of the light guide. The irradiation intensity at the sample pans, measured using an Ocean Optics (USA) USB2000 fibre optic spectroradiometer, was 12.7 mW cm^{-2}. Sample masses of approximately 3mg were used. The calorimeter was calibrated for temperature and enthalpy using high purity zinc and indium standards.

The measured heat flow is proportional to the conversion rate, so that the rate of conversion ($d\alpha/dt$) can be defined as follows:

$$\frac{d\alpha}{dt} = \frac{1}{\Delta H_{tot}}\left(\frac{dH}{dt}\right)_T \quad (1)$$

where $(dH/dt)_T$ is the measured heat flow at a constant temperature T, and ΔH_{tot} is the total exothermic heat of reaction. On the basis of the heat of polymerization for methacrylate groups of 54.4 kJ/mol for the methyl methacrylate [55], the theoretical heat for complete of polymerization of the TEGDMA, NEGDMA, and DEBPADMA monomers were calculated as 380 J/g, 198 J/g, and 241 J/g. respectively. These values were used to calculate the conversion rate and the conversion which was obtained by integrating Equation 1.

2.3. UV-Visible spectrometer

A Cary 3000-Bio (Varian) spectrometer was used to observe the spectroscopic changes in fully formulated resin systems during irradiation with the Polilight PL400. The resin was contained in thin cells (approx. 1 mm thick) constructed of two quartz microscope slides separated by a rubber gasket – this thickness ensured that the radiation was not significantly attenuated by CPTXO absorption through the material. Oxygen was not removed from the resin before irradiation. An identical cell containing ethanol was used as the reference. The distance between the Polilight PL400 and resin during irradiation was 32mm, so that the intensity of the radiation at the surface of the resin was measured to be approximately equal to the intensity of the radiation of the base of the DSC pans. Although the temperature of the photo-DSC experiments (50°C) were higher than in the spectroscopy studies (~20°C), previous studied have shown that the effect of this temperature difference causes a factor of less than two in rates and times of polymerization[50, 56] and so the kinetics of the spectral changes in the UV-vis region and the DSC curing should be comparable.

Results and Discussion

Photo-DSC

The isothermal photocuring behaviours of the TEGDMA/CPTXO, TEGDMA/CPTXO/TMA, TEGDMA/CPTXO/Ph_2IPF_6, and TEGDMA/CPTXO/TMA/Ph_2IPF_6 systems using 415 nm Polilight radiation at 50 °C are presented in Figure 1. In each case, a shoulder appears on the rate curve prior to the maximum. In previous studies of the photopolymerization of TEGDMA and other oligomers by the photoredox radical initiating system, camphorquinone/TMA, this behaviour was interpreted in terms of the complex effects of diffusion control on the polymerization rate constants rather than an effect of the photoinitiation step [50]. Integration of the DSC curves shows that the smallest extent of reaction, indicated by the total heat evolved (ΔH), occurred for TEGDMA/CPTXO (ΔH~10 J/g, see Table 1). In contrast, in another study where camphorquinone was used as the photoinitiator, the TEGDMA/CQ system evolved 220 J/g [41]. Thioxanthones, such as CPTXO, are normally used in cationic polymerization [15,51,52] as photosensitizers which are oxidized by an onium salt, resulting in the formation of cations as well as radicals from the decomposition of the onium salt [15]. Thus when used alone, CPTXO is not expected to be very effective as is demonstrated in Figure 1, and it appears that CPTXO is not able to be readily reduced by monomer and so produces few radicals. However, the CPTXO/Ph_2IPF_6 system cured well (ΔH = 252 J/g) due to the radicals formed by the photo-redox reaction as noted above. The data in Figure 1 for the TEGDMA/CPTXO/TMA system also shows that when used in conjunction with amine, CPTXO is produces effective radicals, presumably by the photo-redox reaction between the excited CPTXO and TMA, and this resulted in a total heat of polymerization of 225 J/g. However, the most efficient initiation system was that of TEGDMA/CPTXO/TMA/Ph_2IPF_6, which gave the highest heat of polymerization (269 J/g). Since the theoretical heat for complete of polymerization of

TEGDMA is 380 J/g (see above), the heat of polymerization of 269 J/g corresponds to 71% conversion of methacrylate groups, and this incomplete conversion is probably due to vitrification of the network during cure at 50°C, which prevents complete polymerization. [57, 58] This explanation is consistent with the measured glass transition temperature of the cured TEGDMA (approx. 140°C based on the maximum in tanδ at 1 Hz [59]) which is well above the isothermal cure temperature.

Inspection of Figure 1 reveals considerable differences in the rates of polymerization for each system. The photopolymerization of TEGDMA with CPTXO/TMA/Ph_2IPF_6 was much faster than CPTXO/Ph_2IPF_6 which was faster than with the CPTXO/TMA system and all were much faster than when CPTXO was used alone. In quantitative terms, the maximum heat flow of 13.6 W/g for TEGDMA/CPTXO/TMA/Ph_2IPF_6 was much greater than TEGDMA/CPTXO/Ph_2IPF_6 (3.8 W/g) or TEGDMA/CPTXO/TMA (1.8 W/g) or TEGDMA/CPTXO (0.12 W/g). The approximately four-fold increase in polymerization rate obtained with the three-component system is very significant because the rate is usually proportional to the square root of the photosensitizer concentration [12] and so a 16-fold increase in CPTXO concentration would normally be required for a similar result.

The influence of the three-component initiation systems on the photo-DSC curing behaviour of the more flexible monomer, NEGDMA, was also investigated and this is presented in Figure 2. NEGDMA/CPTXO/TMA gave a heat of polymerization 158 J/g, but the other two systems had very similar values of 190±10 J/g. The theoretical heat of polymerization of NEGDMA is 198 J/g so that the heat of polymerization of 190 J/g is equivalent to 96% conversion of methacrylate groups which is considerably greater than that found for TEGDMA (about 70% as discussed above). NEGDMA has a much more flexible backbone and polymerizes to a network with a lower glass transition temperature (15 °C, from DMTA at 1 Hz [60]) compared with TEGDMA (140°C [59]). Thus NEGDMA does not

vitrify during cure, thus allowing almost complete conversion. The shape of the photopolymerization curves are similar and show an initial shoulder in the rate before the maximum, as discussed above for TEGDMA (Figure 1). As with TEGDMA, the NEGDMA/CPTXO/TMA/Ph_2IPF_6 system exhibits a significant photopolymerization enhancement with a maximum heat flow of 11.1 W/g compared with the maximum heat flow of 2.0 W/g for NEGDMA/CPTXO/TMA and 3.1 W/g for NEGDMA/CPTXO/Ph_2IPF_6. Thus these results show that the observed major enhancement in photopolymerization rate for the three component systems is not related to whether the monomer forms an elastomer or a glass.

To determine if this photopolymerization enhancement only occurred with aliphatic monomers, the photopolymerization of the aromatic dimethacrylate, DEBPADMA, was also investigated and these data are presented in Figure 3. The DEBPADMA/CPTXO/Ph_2IPF_6 system had a lower polymerization heat (ΔH=107 J/g) but the other systems yielded heats of polymerization of 150±10 J/g. The theoretical heat of polymerization of DEBPADMA is 241 J/g and so the maximum heat of polymerization of 150 J/g corresponds to 62% conversion of methacrylate groups. As with TEGDMA, this low conversion is due to vitrification during cure, which prevents complete polymerization [57, 58] because the glass transition temperature of the cured DEBPADMA (189 °C [61]) is well above the isothermal cure temperature. As noted above, the shape of the photopolymerization curve can have a dependency on the monomer structure [50], and in agreement with previous studies of DEBPADMA/CQ/TMA [50, 56], the photopolymerization of DEBPADMA/CPTXO/TMA, DEBPADMA/CPTXO/Ph_2IPF_6, and DEBPADMA/CPTXO/TMA/Ph_2IPF_6 showed a single maximum in the rate. As found with TEGDMA and NEGDMA, Figure 5 reveals a significant photopolymerization enhancement for the three component initiator system – DEBPADMA/CPTXO/TMA/Ph_2IPF_6 had a maximum heat flow of 15.1 W/g compared with

7.9 W/g for DEBPADMA/CPTXO/TMA and 4.0 W/g for DEBPADMA/CPTXO/Ph_2IPF_6. Thus the efficiency of the three component initiator system is far superior to the single or two component systems, irrespective of the monomer aromaticity.

The efficiency of the CPTXO/amine photoinitiating system might be expected [62, 63] be dependent on the ease with which the amine can donate an electron (which is presumably related to its ionization potential) to the reduced CPTXO. Since the amine, TMA, used in the studies discussed above is a tertiary aromatic amine, it is also worthwhile to study the effect of tertiary semi-aromatic and aliphatic amines on this photopolymerization enhancement. For this, we chose to study two other amines which have different ionization potentials [64] than TMA(7.30±0.02 eV), DMBA (7.69±0.05 eV) and TEA (7.15±0.1 eV). Figure 4 illustrates the isothermal photocuring behavior of the TEGDMA/CPTXO/DMBA, TEGDMA/CPTXO/Ph_2IPF_6 and TEGDMA/CPTXO/DMBA/Ph_2IPF_6 while Figure 5 gives the behaviour for TEGDMA/CPTXO/TEA, TEGDMA/CPTXO/Ph_2IPF_6, and TEGDMA/CPTXO/TEA/Ph_2IPF_6. In comparison with TEGDMA/CPTXO/TMA (see Fig 1), the TEGDMA/CPTXO/DMBA and TEGDMA/CPTXO/TEA systems have very low polymerization rates and heats of reaction (see Table 1). The other systems have similar values for the heat of polymerization (ΔH=270±20 J/g). This heat of polymerization corresponds to 74% conversion due to vitrification during cure, which prevents complete polymerization [57, 58] as mentioned above. As found with TMA, the combination of the Ph_2IPF_6 cationic system and the CPTXO/DMBA or CPTXO/TEA initiator systems significantly accelerates the photopolymerization. Thus the maximum heat flow for the TEGDMA/CPTXO/DMBA/Ph_2IPF_6 and TEGDMA/CPTXO/TEA/Ph_2IPF_6 systems are 15.8 W/g and 23.1 W/g respectively compared with 0.2 W/g, 0.7 W/g and 3.8 W/g for TEGDMA/CPTXO/DMBA, TEGDMA/CPTXO/TEA and TEGDMA/CPTXO/Ph_2IPF_6 systems, respectively.

Since ionization potentials are measured in a vacuum and not in solution, a more reliable method of estimating the reactivity of the CPTXO/amine systems is via use of the Rhem-Weller equation[65, 66] (see Table 2). From this equation, the change in free energy for the photoredox reaction of the CPTXO/TMA and CPTXO/TEA systems was calculated to be -52.2 kJ/mol and -50.3 kJ/mol, respectively, and thus photo-induced electron transfer reaction is thermodynamically favorable when CPTXO acts as electron acceptor from either TMA or TEA. Unfortunately no data has been located in the literature for DMBA. In a similar manner, the free energy for the CPTXO/Ph_2IPF_6 system was calculated to be -103.4 kJ/mol, and so the CPTXO/Ph_2IPF_6 system is also thermodynamically feasible in the photo-induced electron transfer reaction when CPTXO acts as an electron donor. These results are qualitatively, but not quantitatively consistent, with the observed rapid photopolymerization for these systems (see Figures 1 and 5).

Similar photopolymerization behaviour of NEGDMA (Figure 6) and DEBPADMA (Figure 7) was observed when DMBA was used as the amine component of the free radical initiating system (i.e. CPTXO/DMBA). As can be calculated from the data in Table 1, NEGDMA and DEBPADMA were cured to approximately 100% and 55%, respectively. The use of the aliphatic DMBA in three component initiator systems for the cure of NEGDMA also accelerated the cure to the same extent as found with TMA (Table 1). Similarly for DEBPADMA, the three component photoinitiator systems containing DMBA showed enhanced polymerization rates over the two component photoinitiator systems, but the maximum heat flow was less than that found when TMA was used (See Table 1).

Spectroscopic Studies and Reaction Mechanism

The photo-DSC experiments clearly indicate that each of the three components in the CPTXO/amine/Ph_2IPF_6 initiating system plays a different role in the photocuring reaction as

shown by the synergism of the combination of components. In order to understand how the amine and iodonium salt affect the consumption of the photosensitive component (CPTXO), spectroscopic studies were undertaken as a function of irradiation time.

Individual measurements of the UV spectra of the components showed CPTXO strongly absorbed at 270, 315 and 390 nm, while much weaker absorptions were observed by Ph_2IPF_6 at 230 and 255 nm. Unfortunately, impurities in TMA gave a strong absorption at wavelengths less than 330nm and TEGDMA started to strongly absorb below 290nm and so an analysis of the spectral changes below 350nm was not attempted. Figure 8 shows that during the irradiation of 0.2%CPTXO/0.3%TMA in TEGDMA, the spectrum changes dramatically with a decrease in absorption particularly at 385nm, particularly in the first 60s due to reduction of the ketone group in CPTXO, as discussed below. As the absorbance at 385nm decreases, a broader absorption process increases in this region – the reason for this is not understood but is may be caused by the CPTXO radical (which can conjugate with the adjacent phenyl rings making it more stable and also absorb in the visible region) or its by-products. Scheme 2 provides a proposed mechanism for the loss of CPTXO due to the electron transfer mechanism for the photosensitization of CPTXO/TMA, and this is consistent with studies of other ketone-amine systems [12, 18, 67-69, 70].

Figure 9 illustrates the changes in the UV-vis spectra of 0.2% CPTXO/0.3% TMA/1% Ph_2IPF_6 in TEGDMA during irradiation for various intervals at 20 °C. Spectra of similar appearance were observed during the irradiation of the TEGDMA/CPTXO/Ph_2IPF_6 system (i.e., in the absence of TMA). As the absorbance at 385nm decreases, this peak splits into a peak at 370nm with a broad underlying peak similar to that observed for CPTXO/TMA (see Fig 8). As discussed above, this may be due to the absorption spectra of the CPTXO ketyl radical or its by-products. At the same time that the CPTXO is consumed, a new absorbance appears at 500 nm which increases in magnitude with irradiation time, particularly during the

first 200s of irradiation as discussed below. We have observed a similar red-shift when CPTXO/Ph_2IPF_6 was used for cationic polymerization of vinyl ethers and ascribed it to the production of the CPTXO ketone radical cation [52] which may be relatively stable because it is resonance stabilized by the aromatic rings. This conclusion is also supported by the spectroscopic studies of Fouassier et al. [71] for the photoredox reaction of chlorothioxanthone with iodonium ions and several other studies have suggested this [72, 73]. Thus it appears that the excited CPTXO molecule forms an exciplex with Ph_2I^+, and this complex decomposes irreversibly by an electron-transfer mechanism[74-78], to form a thioxanthone radical cation absorbing at 500nm (see Schemes 3 and 4) plus initiating radicals.

Thus, in the CPTXO/TMA/Ph_2IPF_6 system (see Scheme 4), CPTXO is photobleached at 385nm by reaction with the TMA or Ph_2IPF_6 but the reaction product from CPTXO and Ph_2IPF_6 causes photodarkening at 500 nm. Such photodarkening behavior is normally unwanted, particularly in composites, because it diminishes the curing of deeper layers of resin. However in the current system, the new peak at 500nm is not overlapped with the CPTXO peak and so this process merely causes a visible color change of the cured product.

In order to quantitatively compare the photobleaching kinetics of different systems, the extent of CPTXO consumption was calculated from the ratio A/A_0, where A is the absorbance at a given time and A_0 is the absorbance before irradiation, and this data is presented in Figure 10. TMA and Ph_2IPF_6 are in excess of CPTXO by factors of three-fold and five-fold, respectively, so that if there is only one main mechanism for the reduction of CPTXO by amine (Scheme 2) and for the oxidation (Scheme 3) of CPTXO by Ph_2IPF_6, then the rate of its consumption can be assumed to be given by the first order expressions[79]:

$$[CPTXO] = [CPTXO]_0 \exp(-k_1 [TMA] t) \qquad \text{Eqn.1}$$

$$[CPTXO] = [CPTXO]_0 \exp(-k_2 [Ph_2IPF_6] t) \qquad \text{Eqn.2}$$

where k_1 and k_2 are the rate constants for CPTXO reduction and oxidation, respectively. Figure 10 illustrates the photobleaching kinetics at 385 nm for the different photoinitiator systems, and shows that CPTXO in the TEGDMA/CPTXO/TMA system undergoes a fast degradation with a first order exponential decay time constant (the reciprocal of k_1) of 32±2 s. The rates of photobleaching for the other two systems are much slower - TEGDMA/CPTXO/Ph_2IPF_6 with a time constant (the reciprocal of k_2) of 220±40 s and TEGDMA/CPTXO/TMA/Ph_2IPF_6 with a time constant of 260±40 s. The slower rate of CPTXO photobleaching for the TEGDMA/CPTXO/Ph_2IPF_6 and TEGDMA/CPTXO/TMA/Ph_2IPF_6 systems compared with the TEGDMA/CPTXO/TMA system suggests that the iodonium salt interferes with the loss of CPTXO or regenerates it (see Schemes 3 and 4). In fact the data for these TEGDMA/CPTXO/Ph_2IPF_6 and TEGDMA/CPTXO/TMA/Ph_2IPF_6 systems are better fit (not shown in Figure 10) by two first order exponentials, and this may be due to reactions leading to the regeneration of CPTXO from its radical cation. One way in which this could occur is by reduction of the CPTXPO radical cation by monomer (see Scheme 3) or TMA (see Scheme 4), as discussed below.

The photodarkening behaviour at 500nm due to the formation of the CPTXO cation radical occurs primarily during the first 50 to 200s, and is shown in Figure 11 for the different photoinitiator systems. The formation of this ketyl radical cation is faster in the TEGDMA/CPTXO/Ph_2IPF_6 system than in the TEGDMA/CPTXO/TMA/Ph_2IPF_6 system and does not occur for the TEGDMA/CPTXO/TMA system. However, unlike the rate of loss of the CPTXO (see above), the kinetics involved in the formation of the CPTXO radical cation are very poorly fitted to a single first order reaction (not shown in Figure 11). This may be due to the kinetics being dependent on both the rate of formation (see Equation 3) and consumption of the CPTXO radical cation (see Equation 4):

$$CPTXO^* + Ph_2IPF_6 \xrightarrow{k_2} CPTXO^+\bullet + Ph\bullet + PhI \quad \text{Eqn. 3}$$

$$CPTXO^{+}\bullet + RED \xrightarrow{k_3} CPTXO + RED\bullet + H^{+} \quad \text{Eqn. 4}$$

where RED is monomer (see Scheme 3) in the TEGDMA/CPTXO/Ph_2IPF_6 system or TMA (see Scheme 4) in the TEGDMA/CPTXO/TMA/Ph_2IPF_6 system. Based on the reactions proposed in Equations 3 and 4, the kinetics are reasonably fitted to two pseudo first-order processes[79]:

$$[CPTXO^{+}\bullet] = \frac{k_2\,[CPTXO]_0\,[Ph_2IPF_6]}{k_3\,[RED] - k\,[Ph_2IPF_6]}\left(e^{-k_2[Ph_2IPF_6]} - e^{-k_3[RED]}\right) \quad \text{Eqn. 5}$$

as shown in Figure 11.

Thus the primary photoreaction for the TEGDMA/CPTXO/TMA system (Figure 10), appears to occur between the CPTXO and the TMA (and the monomer to a lesser extent). The proposed mechanism (Scheme 2) involves formation of an exciplex between the tertiary amine/monomer and the photoexcited CPTXO. H-transfer results in the formation of an aminoalkyl radical that initiates polymerization and a non-propagating ketyl radical which can potentially act as a terminator [18, 67-69]. The rate of CPTXO loss is highest for this system (see Fig 10) because the CPTXO reduction product is not regenerated (i.e. oxidized) back to CPTXO. In addition, the TEGDMA/CPTXO/TMA system does not form a colored degradation product at 500nm (see Figure 11) because this photoinitiator system contains no iodonium salt to oxidize the CPTXO.

In contrast, for the CPTXO/Ph_2IPF_6 system, the mechanism shown in Scheme 3 appears to involve the formation of an exciplex between CPTXO and Ph_2I^{+}, followed by the decomposition of the complex by an electron-transfer mechanism to form a thioxanthone radical cation and a phenyl radical as discussed above. In the next step, this thioxanthone radical cation could slowly react with monomer to regenerate CPTXO and also form an alkyl radical via electron transfer. Since the CPTXO could only be slowly regenerated by

monomer, the TEGDMA/CPTXO/Ph_2IPF_6 photobleaching rate should be slower than for the TEGDMA/CPTXO/TMA system as is observed (see Figure 10).

Whereas, for the CPTXO/TMA/Ph_2IPF_6 system, the influence of the onium salt on the photoinitiation reaction can be explained by the mechanisms illustrated in Scheme 4. As discussed above, a thioxanthone radical cation and a phenyl radical are formed by an electron transfer from the photoexcited CPTXO to the iodonium salt. In the next step, we propose this thioxanthone radical cation reacts with TMA (and with monomer to a lesser extent) to regenerate CPTXO and also form an aminoalkyl radical via electron transfer. This newly formed aminoalkyl radical could also initiate polymerization. Due to this CPTXO regeneration, the rate of development in the CPTXO/TMA/Ph_2IPF_6 system of the peak at 500nm, due to the CPTXO cation radical, is slower than for the CPTXO/Ph_2IPF_6 system

The photopolymerization kinetics can also be explained by the mechanisms proposed. In the absence of iodonium salt or amine, the photopolymerization is slow because the charge transfer of the excited CPTXO to monomer is very inefficient and is reversible. When either amine or iodonium salt are present with CPTXO, the excited ketone can be reduced (with amine) or oxidized (with iodonium salt), as suggested by thermodynamic calculations discussed above. These reactions lead to either the production of amine and ketyl radicals from CPTXO/amine system, or phenyl and ketyl radicals from CPTXO/Ph_2IPF_6. The observation that both systems produce similar peak polymerization rates (see Table 1) suggests that the role of the ketyl radical as a terminator of polymerization [18, 67-69] is not very important here. If it had been important, then the rate of photopolymerization with the CPTXO/Ph_2IPF_6 photoinitiator system (where the ketyl radical is not directly formed) would be markedly faster than with CPTXO/TMA (where the CPTXO radical is formed). Also the regeneration of the reacted CPTXO cannot be a dominant feature because the rate of photobleaching and loss of CPTXO during the timescale of the DSC experiments (approx. 60

s) is greatest for the CPTXO/TMA/ Ph_2IPF_6 system and leads to almost 50% loss of the photosensitizer but this is also the fastest photopolymerizing system.

In the three component system (see Scheme 4), it appears that irreversible oxidation of either the ketyl radical (as suggested by Kim and Stansbury[33] for rose-bengal and fluorescein) or of the amine radical (as suggested by Bi and Neckers[42] and by Yagci and Hepuzer[43]) by the iodonium salt is the main cause for the accelerated photopolymerization rate with the three component initiator systems. In the former process (as discussed above), the non-propagating ketyl radical is oxidized by Ph_2IPF_6 to form an active phenyl radical [11], which can also initiate polymerization and could also contribute to the enhanced photopolymerization rate of the three component initiator systems. However for the latter process, the loss of initiating amine radicals through oxidation by the iodonium cation may not have a very detrimental effect on the polymerization rate because the phenyl radical formed in its place can lead to initiating radicals by H-abstraction.

In summary, the Ph_2IPF_6 appears to play four roles. First, it reacts with the photoexcited CPTXO to form an initiating carbon-centred radical. Second, it replaces an inactive and possibly terminating CPTXO ketyl radical with an active, initiating radical, and this is consistent with the original proposal by Yagci et al.[80] that photoinitiation efficiency could be enhanced if terminating radicals are converted into initiating radicals. Third, it causes irreversible generation of radicals formed from the CPTXO-amine and CPTXO-monomer reactions and prevents the back-electron transfer process as suggested for other photoinitiation systems [33, 42, 43, 81, 82]. Finally, it regenerates the CPTXO, a component of the original initiating systems.

Conclusions

The curing kinetics and the initiation mechanism of the three-component CPXTO/amine/Ph_2IPF_6 systems have been investigated by photo-DSC and UV-visible spectroscopy using aromatic (TMA) and aliphatic (DMBA or TEA) tertiary amines as electron donors. Three different monomers with different flexibilities in the backbone, TEGDMA, NEGDMA, and DEBPADM, were also investigated.

The maximum photopolymerization rates of TEGDMA with CPTXO, CPTXO/TMA, CPTXO/Ph_2IPF_6, and CPTXO/TMA/Ph_2IPF_6 systems follows the trend: CPTXO/TMA/Ph_2IPF_6 >> CPTXO/Ph_2IPF_6 > CPTXO/TMA > CPTXO. The increase in the maximum rate for the three component initiator systems was found to be typically a factor of 4. This unexpected result is significant because the rate is usually proportional to the square root of the initiator concentration and so a 16-fold increase in CPTXO concentration would be required for a similar result. The photocuring behavior of initiation systems using the aliphatic tertiary amines DMBA and TEA were similar to that with TMA, suggesting this phenomenon is quite general. In addition, similar results were obtained with the flexible backone monomer, NEGDMA, and the aromatic DEBPADMA monomer, although these polymerized to different conversions, due to a vitrification effect.

Spectroscopic studies revealed CPTXO was consumed during photo-irradiation in the various initiating systems and the rate of CPTXO loss followed trend: CPTXO/TMA >> CPTXO/Ph_2IPF_6 > CPTXO/TMA/Ph_2IPF_6. This is not consistent with the DSC cure kinetics and shows that rapid consumption of CPTXO does not equate to rapid production of initiating radicals. In addition, the TEGDMA/CPTXO/TMA/Ph_2IPF_6 system exhibited the formation of a new absorption peak which was attributed to the CPTXO radical cation. The rate of its development followed the trend: CPTXO/Ph_2IPF_6 > CPTXO/TMA/Ph_2IPF_6 and no photodarkening behavior was found for the CPTXO/TMA system.

Based on these results, three different mechanisms have been proposed. For the CPTXO/TMA initiating system, the mechanism involves formation of an exciplex between the tertiary amine or monomer and the photoexcited CPTXO. Reversible H-transfer results in an aminoalkyl radical that initiates polymerization and a non-propagating ketyl radical which may act as a terminator. For the CPTXO/Ph_2IPF_6 system, the mechanism involves the formation of a thioxanthone radical cation and a phenyl radical by an electron-transfer mechanism, plus oxidation of monomer by CPTXO to form a ketyl radical which is reconverted by the iodonium salt to its original state. For the CPTXO/TMA/Ph_2IPF_6 system, the reaction involves the irreversible formation of a thioxanthone radical cation and a phenyl radical by an electron-transfer mechanism, followed by H-transfer between a thioxanthone radical cation and TMA (or monomer) to regenerate CPTXO, and also the formation of an aminoalkyl radical which is potentially irreversibly oxidized to a amine cation. It is the irreversible nature of these latter two reactions which gives the three component system its photoinitiation efficiency.

Acknowledgements

The authors would like to acknowledge the ARC Discovery grants (DP0453104 and DP1093217) for financial support. Helpful discussions with Professor Yusuf Yagci (Istanbul Technical University) are also gratefully acknowledged.

List of Figures and Tables

Table 1 Summary of results from isothermal photo-DSC of TEGDMA, NEGDMA and DEBPADMA with CPTXO, TMA, DMBA, TEA, and Ph_2IPF_6.

Systems	ΔH (Jg^{-1})	Peak maximum Time (sec)	Peak maximum Heat flow (W/g)
TEGDMA			
TEGDMA- TMA			
TEGDMA/0.2%CPTXO	10	10	0.12
TEGDMA/0.2%CPTXO/0.3%TMA	225	7 and 42	1.8 and 1.6
TEGDMA/0.2%CPTXO/1%Ph_2IPF_6	252	7 and 36	1.8 and 3.8
TEGDMA/0.2%CPTXO/0.3%TMA/1%Ph_2IPF_6	269	20	13.6
TEGDMA- DMBA			
TEGDMA/0.2%CPTXO/0.3%DMBA	12	8	0.2
TEGDMA/0.2%CPTXO/0.3%DMBA/1%Ph_2IPF_6	292	18	15.8
TEGDMA- TEA			
TEGDMA/0.2%CPTXO/0.3% TEA	70	6	0.7
TEGDMA/0.2%CPTXO/0.3% TEA /1%Ph_2IPF_6	288	11	23.1
NEGDMA			
NEGDMA-TMA			
NEGDMA/0.2%CPTXO/0.3%TMA	158	9 and 26	1.6 and 2.0
NEGDMA/0.2%CPTXO/1%Ph_2IPF_6	187	9 and 38	1.4 and 3.1
NEGDMA/0.2%CPTXO/0.3%TMA/1%Ph_2IPF_6	189	17	11.1
NEGDMA-DMBA			
NEGDMA/0.2%CPTXO/0.3%DMBA	25	29	0.1
NEGDMA/0.2%CPTXO/0.3%DMBA/1%Ph_2IPF_6	201	15	10.9
DEBPADMA			
DEBPADMA-TMA			
DEBPADMA/0.2%CPTXO/0.3%TMA	137	7	7.9
DEBPADMA/0.2%CPTXO/1%Ph_2IPF_6	107	9	5.9
DEBPADMA/0.2%CPTXO/0.3%TMA/1%Ph_2IPF_6	147	5	15.1
DEBPADMA-DMBA			
DEBPADMA/0.2%CPTXO/0.3%DMBA	88	9	1.9
DEBPADMA/0.2%CPTXO/0.3%DMBA/1%Ph_2IPF_6	130	7	8.9

* polymerization continuing at the cessation of irradiation

Table 2. Free energy changes of photo-induced electron transfer reactions (ΔG_{et}) with CPTXO calculated from the Rhem-Weller equation [65, 66]:

$$\Delta G_{et} = F\left\{E_{ox}(D/D^{+}\bullet) - E_{red}(A/A^{+}\bullet) - E^{*}\right\}$$

where F is Faraday's constant; $E_{ox}(D/D^{+}\bullet)$ is the oxidation potential of the electron donor for CPTXO and the amines, $E_{ox}(A/A^{+}\bullet)$ is the reduction potential for the electron acceptors CPTXO and Ph_2IPF_6 and E* is the excited state energy of CPTXO (2.84 eV [83]).

	CPTXO oxidation	CPTXO reduction	TMA oxidation	TEA oxidation	DMBA oxidation	Ph_2IPF_6 reduction
Redox potential (V) relative to the Standard Calomel Electrode #	1.57 [83]	-1.66 [84]	0.64 [85]	0.66 [86]	-	-0.2 [87]
ΔG (kJ/mol) for amine reduction or Ph_2IPF_6 oxidation of CPTXO	-	-	-52.2	-50.3	-	-103.4

Oxidation potentials are positive

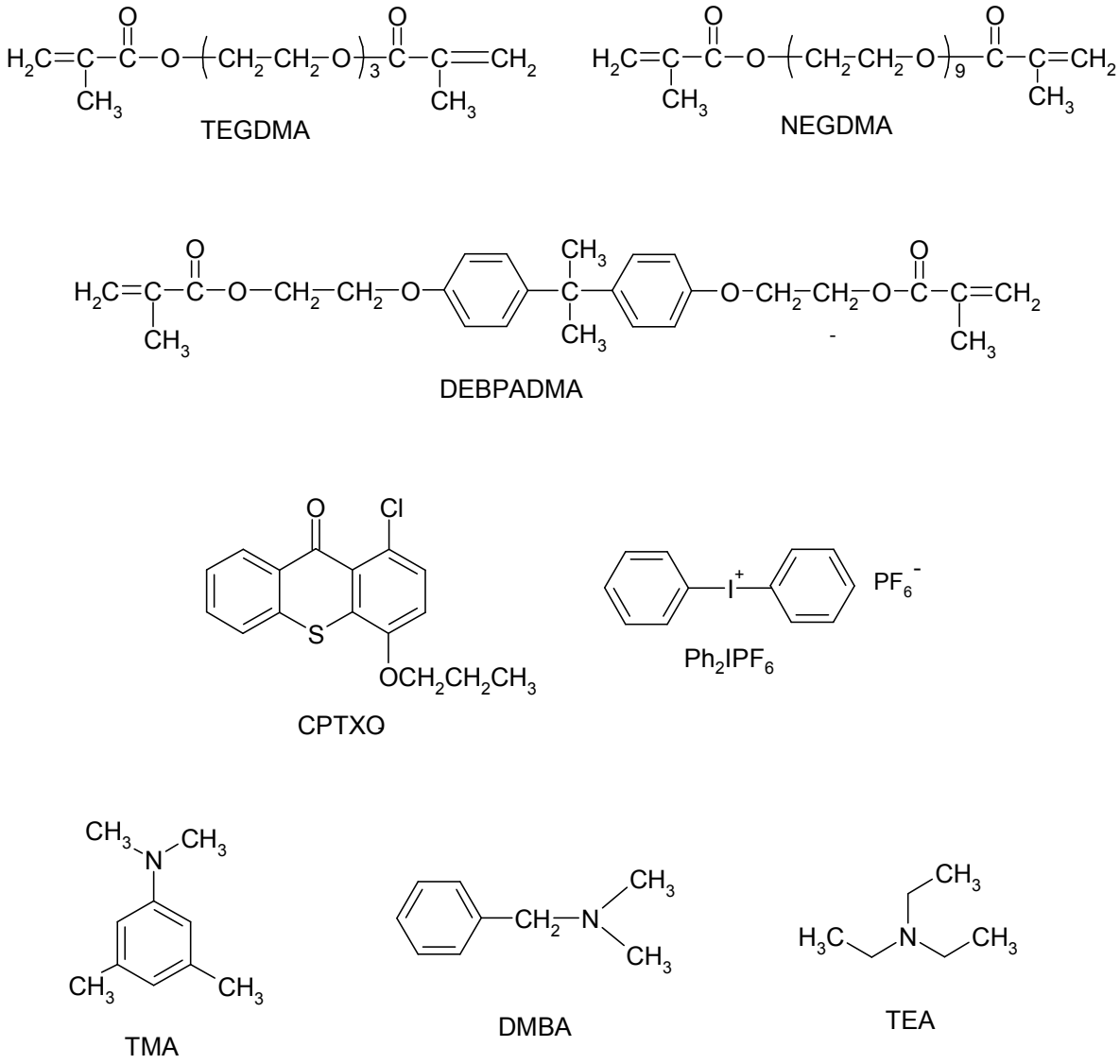

Scheme 1 Molecular structures of monomers, ketones, amines, and onium salts

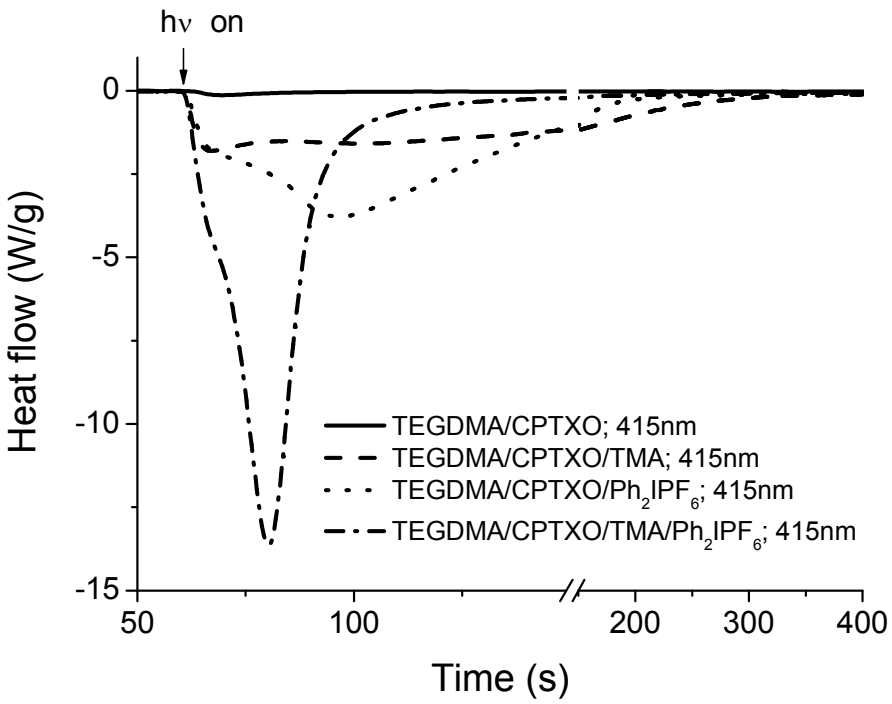

Figure 1 Photocuring of TEGDMA/CPTXO, TEGDMA/CPTXO/TMA, TEGDMA/CPTXO/Ph_2IPF_6, and TEGDMA/CPTXO/TMA/Ph_2IPF_6. The irradiation intensity at the sample pans was 12.7 mW cm^{-2}. The heats of polymerization are 10 J/g, 225 J/g, 252 J/g, and 269 J/g, respectively.

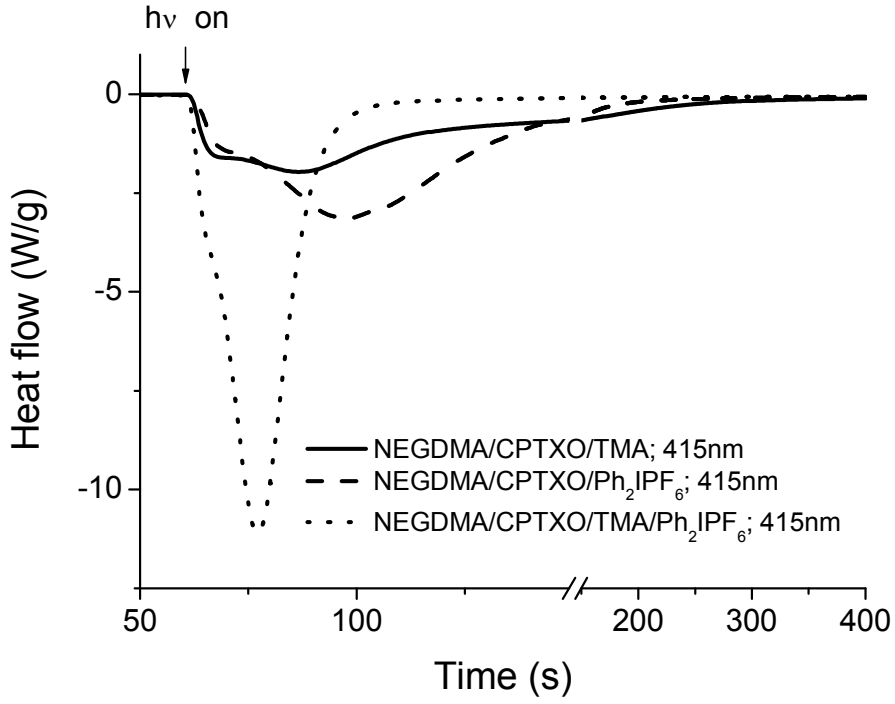

Figure 2 Photocuring of NEGDMA/CPTXO/TMA, NEGDMA/CPTXO/Ph_2IPF_6, and NEGDMA/CPTXO/Ph_2IPF_6/TMA. The irradiation intensity at the sample pans was 12.7 mW cm^{-2}. The heats of polymerization are 158 J/g, 187 J/g and 189 J/g, respectively.

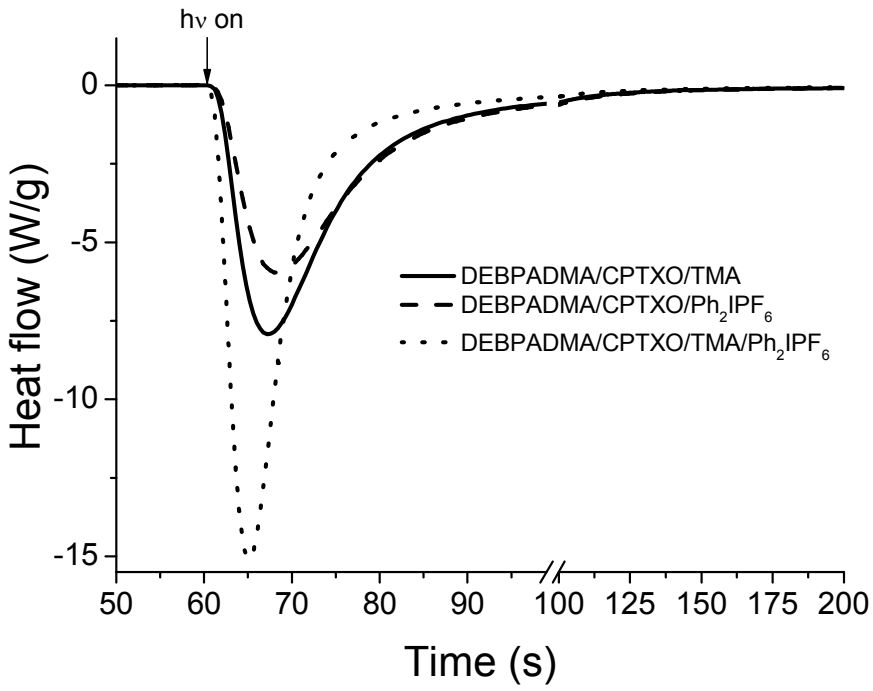

Figure 3 Photocuring of DEBPADMA/CPTXO/TMA, DEBPADMA/CPTXO/Ph_2IPF_6, and DEBPADMA/CPTXO/Ph_2IPF_6/TMA. The irradiation intensity at the sample pans was 12.7 mW cm^{-2}. The heats of polymerization are 137 J/g, 107 J/g and 147 J/g, respectively

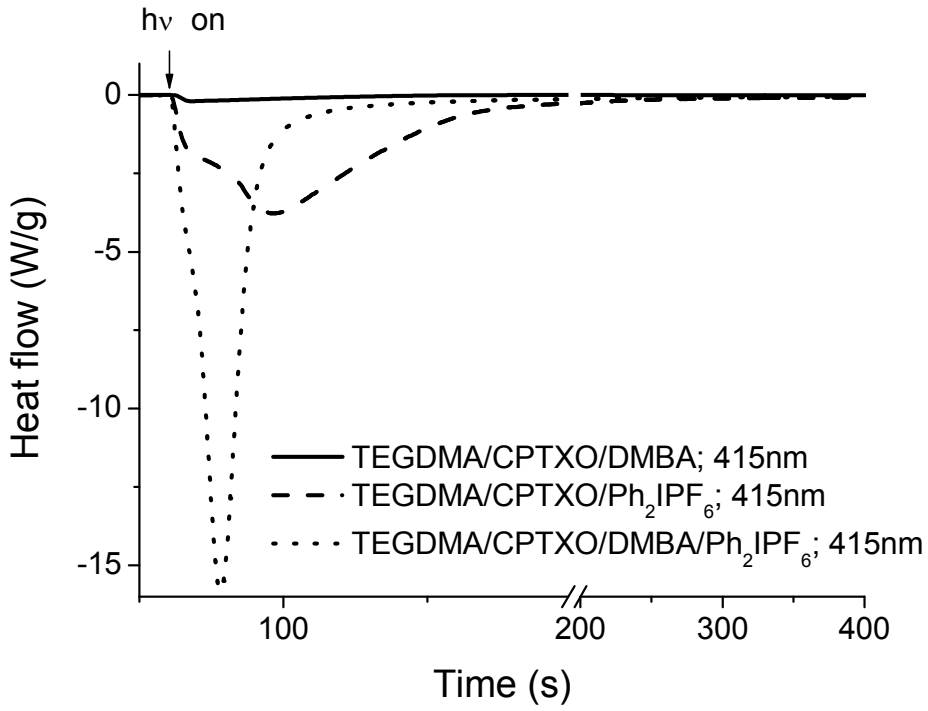

Figure 4 Photocuring of TEGDMA/CPTXO/DMBA, TEGDMA/CPTXO/Ph_2IPF_6 and TEGDMA/CPTXO/DMBA/Ph_2IPF_6. The irradiation intensity at the sample pans was 12.7 mW cm^{-2}. The heats of polymerization are 12 J/g, 252 J/g and 292 J/g, respectively.

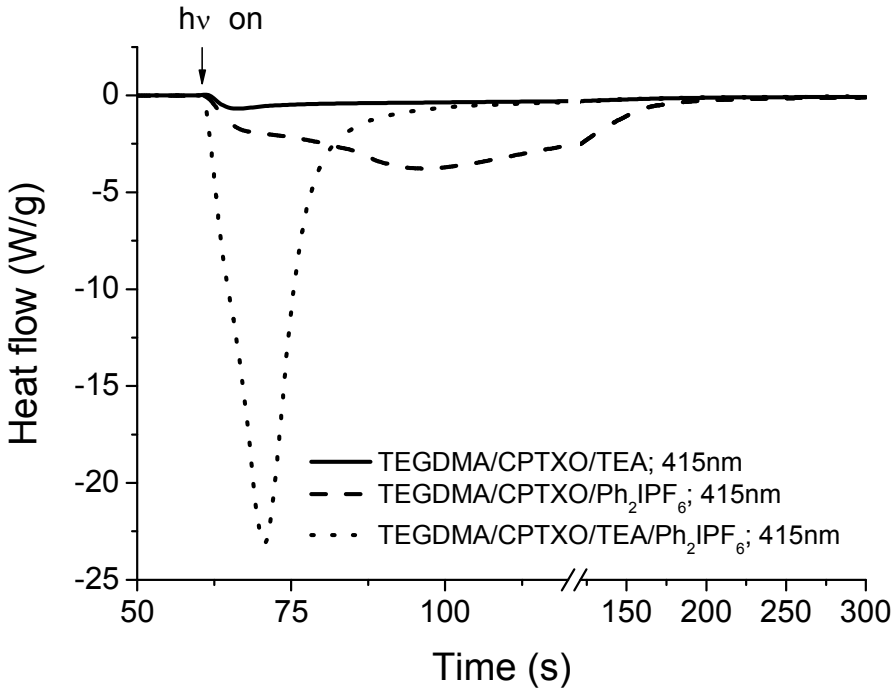

Figure 5 Photocuring of TEGDMA/CPTXO/TEA, TEGDMA/CPTXO/Ph_2IPF_6, and TEGDMA/CPTXO/TEA/Ph_2IPF_6. The irradiation intensity at the sample pans was 12.7 mW cm^{-2}. The heats of polymerization are 70 J/g, 252 J/g, and 288 J/g, respectively.

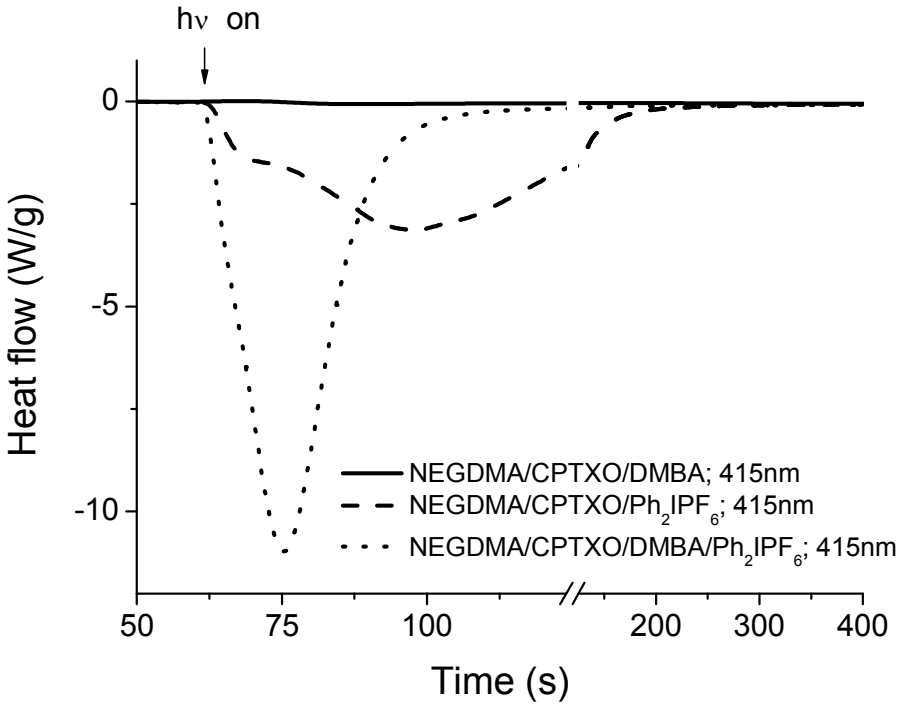

Figure 6 Photocuring of NEGDMA/CPTXO/DMBA, NEGDMA/CPTXO/Ph_2IPF_6, and NEGDMA/CPTXO/DMBA/Ph_2IPF_6. The irradiation intensity at the sample pans was 12.7 mW cm^{-2}. The heats of polymerization are 25 J/g, 187 J/g, and 201 J/g, respectively.

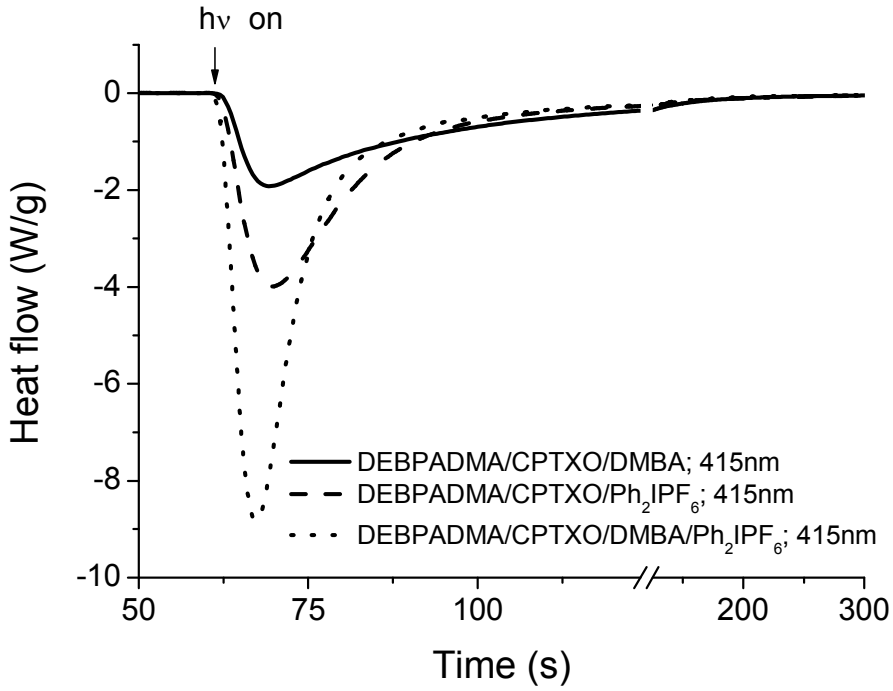

Figure 7 Photocuring of DEBPADMA/CPTXO/DMBA, DEBPADMA/CPTXO/Ph_2IPF_6, and DEBPADMA/CPTXO/DMBA/Ph_2IPF_6. The irradiation intensity at the sample pans was 12.7 mW cm^{-2}. The heats of polymerization are 88 J/g, 107 J/g, and 130 J/g, respectively.

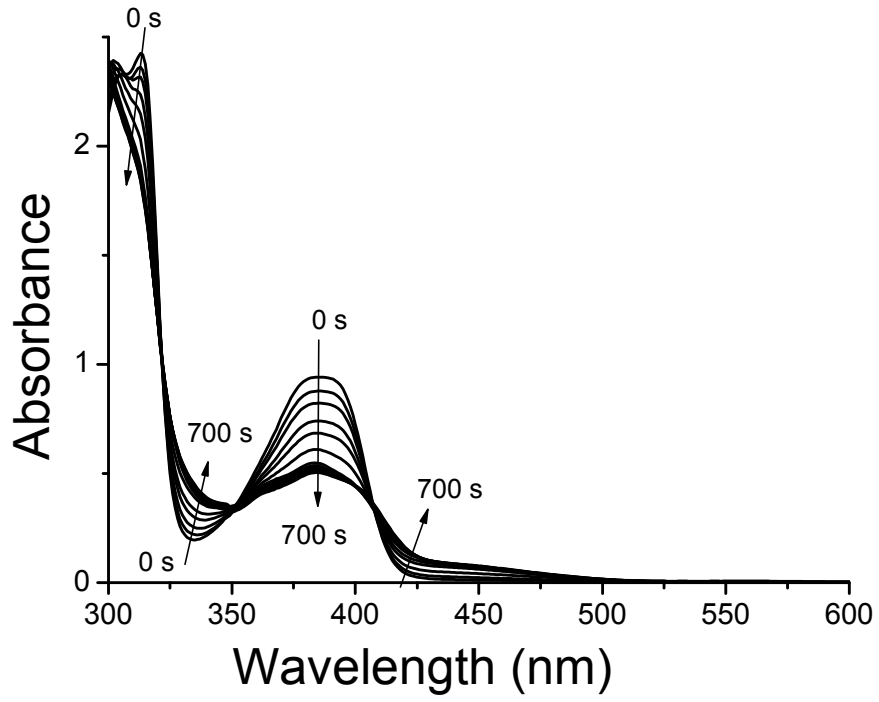

Figure 8 UV-Visible absorption spectra of TEGDMA/0.2%CPTXO/0.3%TMA using a path length of 0.4 mm irradiated with ~ 13 mW cm^{-2} at 415 nm for various intervals (0 ~ 11.5min) at 20 °C

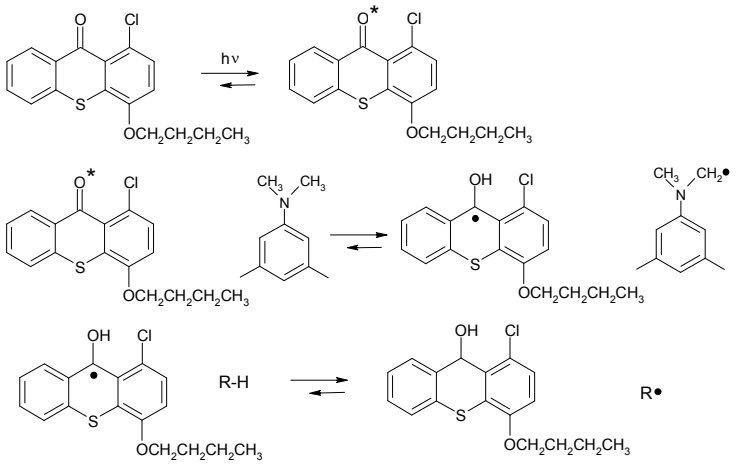

Scheme 2 The reversible electron transfer mechanism for the photosensitization of CPTXO/TMA

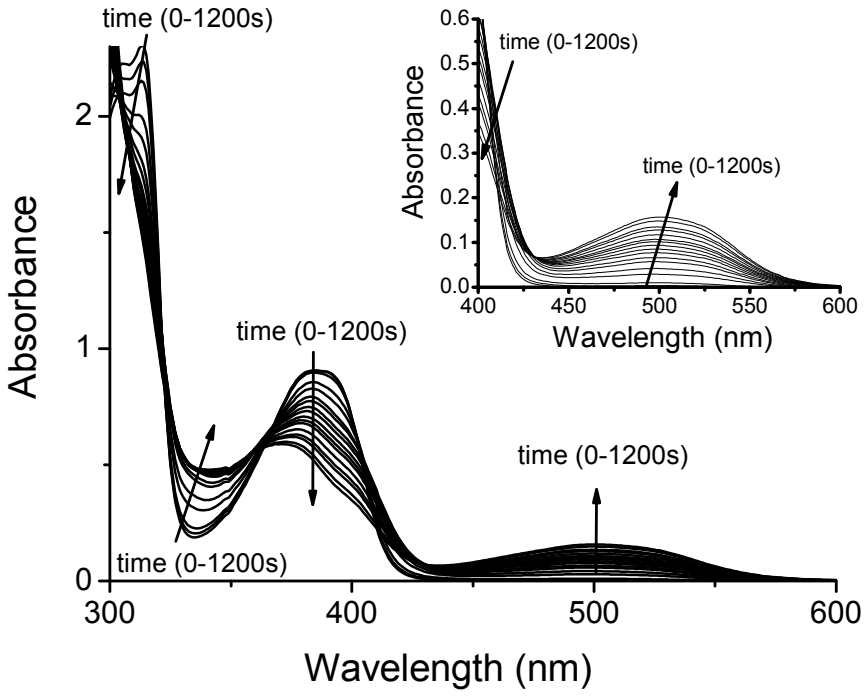

Figure 9 UV-Visible absorption spectra of TEGDMA/0.2%CPTXO/0.3%TMA/1% Ph_2IPF_6 using a path length of 0.4 mm irradiated with ~ 13 mW cm^{-2} at 415 nm for various intervals (0 ~ 19.5min) at 20 °C.

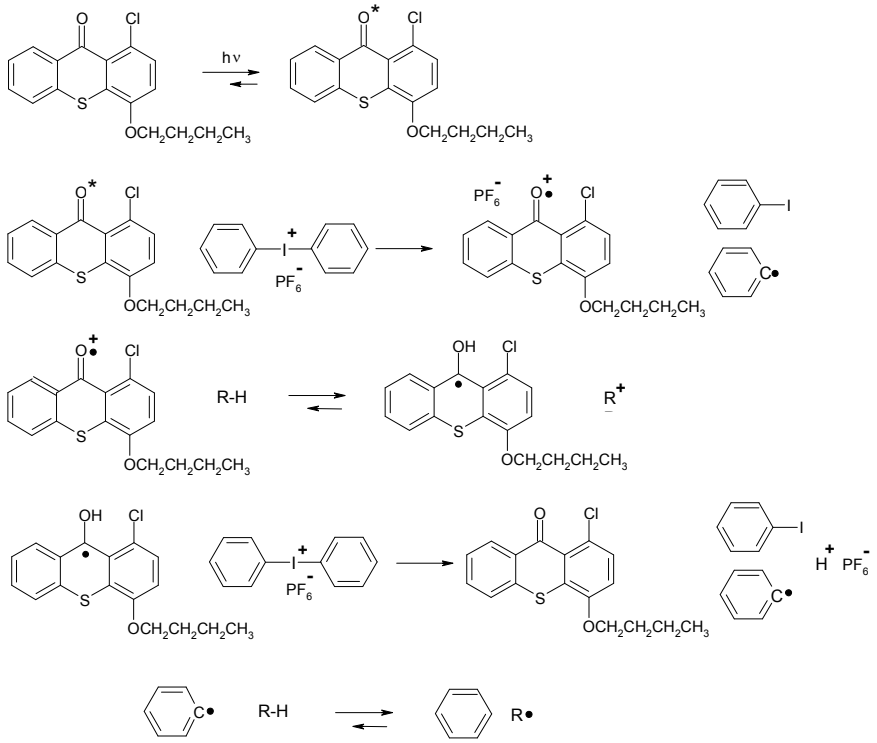

Scheme 3 The electron transfer mechanism for the photosensitization of CPTXO/Ph_2IPF_6 which leads to partial CPTXO regeneration by monomer (R-H) and Ph_2IPF_6. Note that the second and fourth reactions are considered to be essentially irreversible.

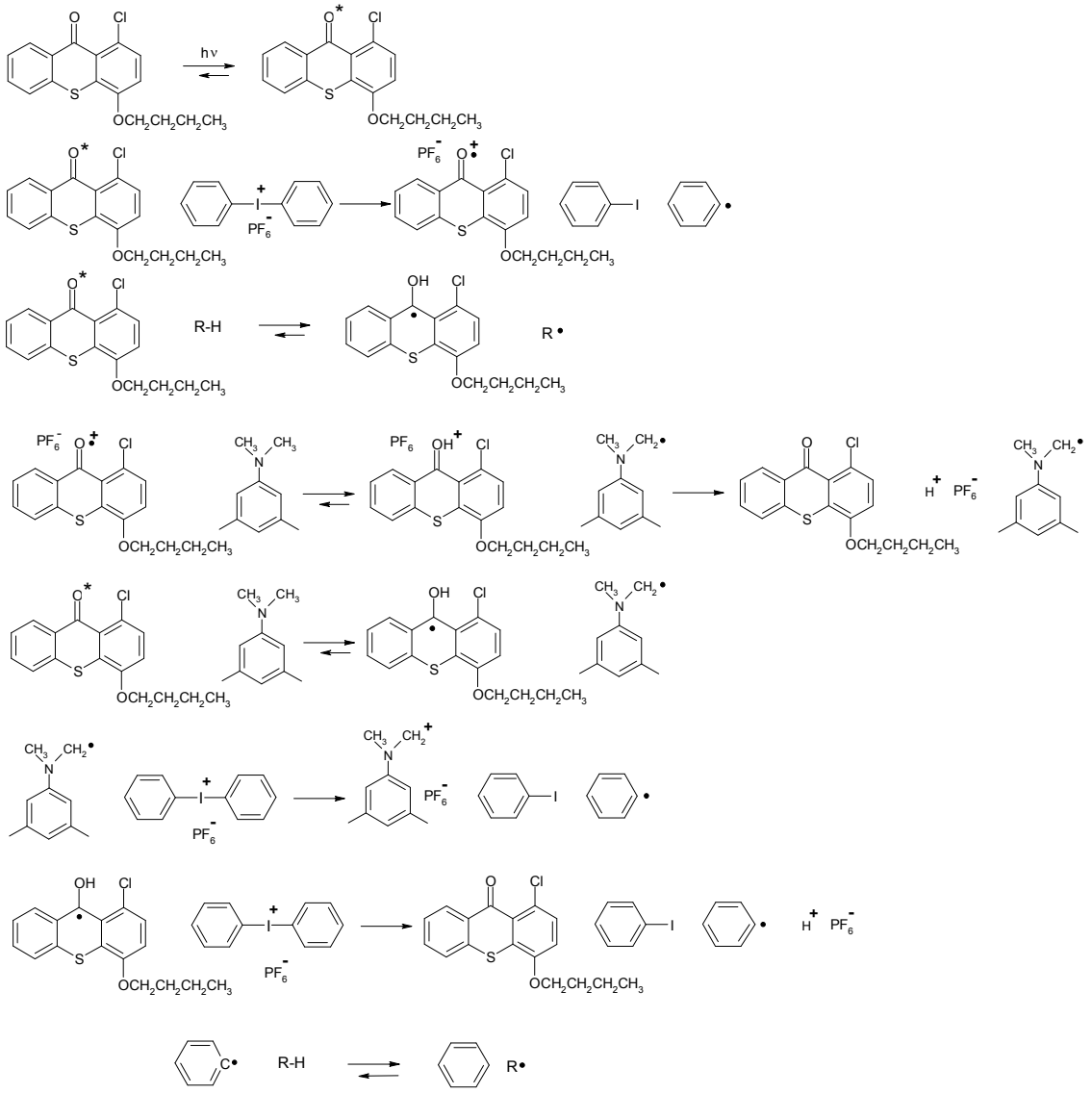

Scheme 4 Parallel-sequential photoinitiation mechanism for CPTXO/TMA/Ph_2IPF_6 which leads to limited CPTXO regeneration and also slow photodarkening. Note that the second and sixth reactions are considered to be essentially irreversible.

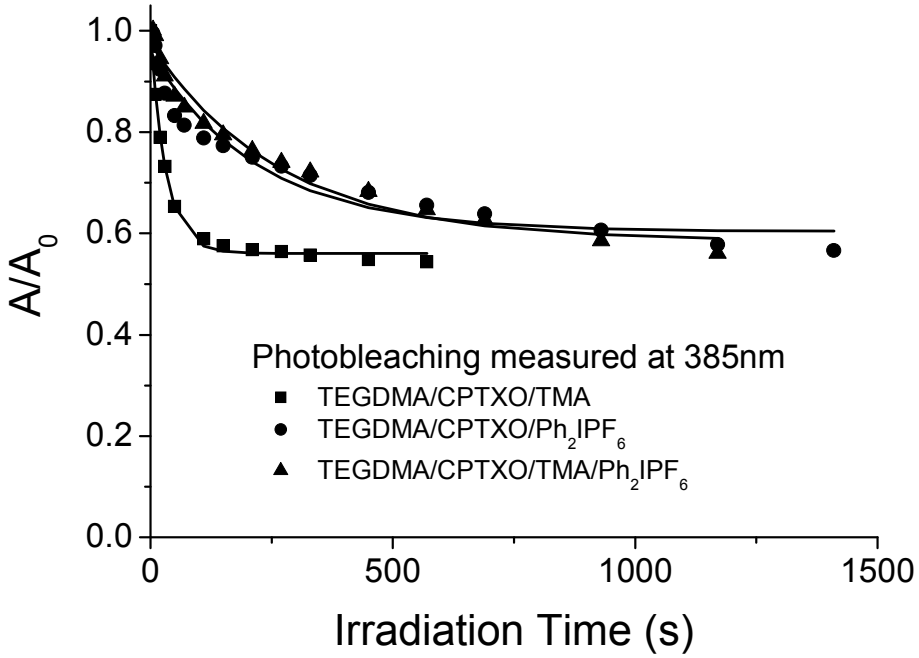

Figure 10 Photobleaching kinetics of CPTXO in TEGDMA/CPTXO/TMA, TEGDMA/CPTXO/Ph_2IPF_6, and TEGDMA/CPTXO/TMA/Ph_2IPF_6, measured at 385nm. The solid lines are first order fits to the consumption of the CPTXO.

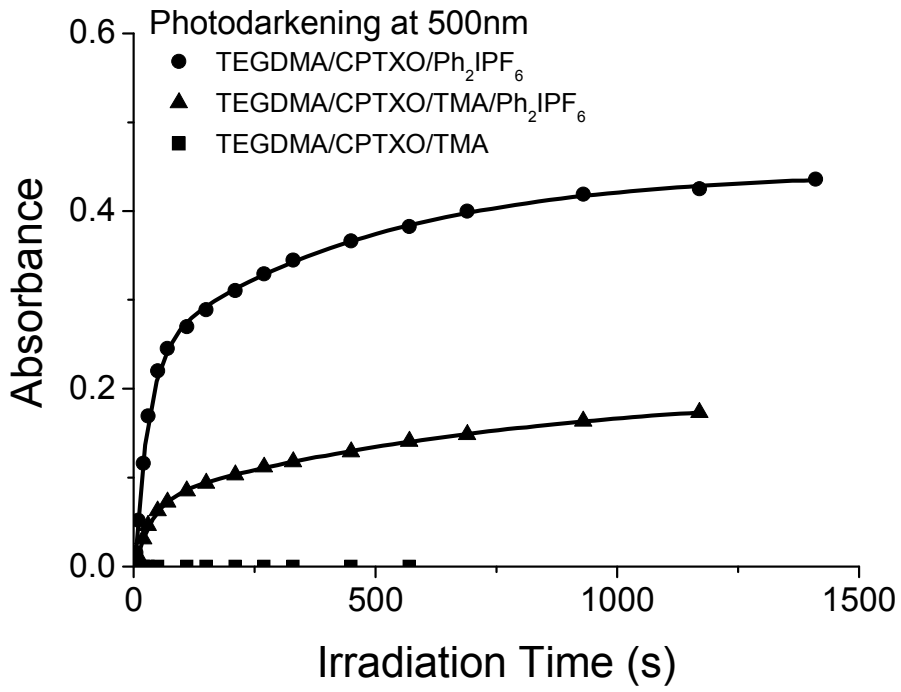

Figure 11 Photodarkening kinetics of TEGDMA/CPTXO/Ph_2IPF_6, TEGDMA/CPTXO/TMA and TEGDMA/CPTXO/TMA/Ph_2IPF_6, measured at 500nm. The solid lines are double exponential fits to the data. Note that no absorption at 500nm appeared for TEGDMA/CPTXO/TMA system.

References

1. J.-P. Fouassier, *Photoinitiation, Photopolymirization and Photocuring: Fundamentals and Applications*, Hanser Gardner Publicaions, Cincinnati, OH, 1995.
2. C. G. Roffey, *Photopolymerization of Surface Coatings*, John Wiley and Sons Led., New York, 1982.
3. P. Dufour, *State-of-the-Art and Trends in the Radiation-Curing Market*, Elsevier Applied Science, London, 1993.
4. J.-P. Fouassier, *Photoinitiated Polymerization: Theory and Applications*, Rapra Technology Ltd., Shawbury, 1998.
5. Z. Kucybala, M. Pietrzak, J. Paczkowski, L. A. Linden and J. F. Rabek, *Polymer*, 1996, **37**, 4585-4591.
6. K. S. Padon and A. B. Scranton, *Recent Res. Dev. Polym. Sci.*, 1999, **3**, 369-385.
7. K. S. Anseth, A. T. Metters, S. J. Bryant, P. J. Martens, J. H. Elisseeff and C. N. Bowman, *J. Controlled Release*, 2002, **78**, 199-209.
8. J. V. Koleske, *Radiation Curing of Coatings*, West Conshohocken, PA, 2002.
9. G. A. Miller, L. Gou, V. Narayanan and A. B. Scranton, *J. Polym. Sci., Part A: Polym. Chem.*, 2002, **40**, 793-808.
10. D. F. Eaton, in *Advances in Photochemistry*, John Wiley & Sons, Inc., 2007, pp. 427-487.
11. J. P. Fouassier, D. Ruhlmann, Y. Takimoto, M. Harada and M. Kawabata, *J. Polym. Sci., Part A: Polym. Chem.*, 1993, **31**, 2245-2248.
12. W. D. Cook, *Polymer*, 1992, **33**, 600-609.
13. G. Yilmaz, A. Tuzun and Y. Yagci, *Journal of Polymer Science, Part A: Polymer Chemistry* 2010, **48**, 5120-5125.
14. J. Lalevee, N. Blanchard, M. A. Tehfe, C. Fries, F. Morlet-Savary, D. Gigmes and J. P. Fouassier, *Polymer Chemistry*, 2011, **2**, 1077-1084.
15. J. V. Crivello and M. Sangermano, *J. Polym. Sci., Part A: Polym. Chem.*, 2001, **39**, 343-356.
16. U. Bulut, G. E. Gunbas and L. Toppare, *Journal of Polymer Science Part A: Polymer Chemistry*, 2010, **48**, 209-213.
17. D. Kim and A. Scranton, *J. Polym. Sci., Part A: Polym. Chem.*, 2004, **42**, 5863-5871.
18. K. S. Padon and A. B. Scranton, *J. Polym. Sci., Part A: Polym. Chem.*, 2000, **38**, 2057-2066.
19. K. S. Padon and A. B. Scranton, *J. Polym. Sci., Part A: Polym. Chem.*, 2001, **39**, 715-723.
20. K. S. Padon and A. B. Scranton, *J. Polym. Sci., Part A: Polym. Chem.*, 2000, **38**, 3336-3346.
21. J.-P. Fouassier, A. Erddalane, F. Morlet-Savary, I. Sumiyoshi, M. Harada and M. Kawabata, *Macromolecules*, 1994, **27**, 3349-3356.
22. M. Harada, Y. Takimoto, N. Noma and Y. Shirota, *J. Photopolym. Sci. Technol.*, 1991, **4**, 51-54.
23. M. Kume, Y. Ohe and T. Taguchi, *J. Photopolym. Sci. Technol.*, 1999, **12**, 185-188.
24. X. Allonas, J. P. Fouassier, M. Kaji, M. Miyasaka and T. Hidaka, *Polymer*, 2001, **42**, 7627-7634.
25. M. L. Gomez, V. Avila, H. A. Montejano and C. M. Previtali, *Polymer*, 2003, **44**, 2875-2881.
26. S. C. Clark, D. J. T. Hill, C. E. Hoyle, S. Joensson, C. W. Miller and L. Y. Shao, *Polym. Int.*, 2003, **52**, 1701-1710.
27. T. B. Cavitt, B. Phillips, C. E. Hoyle, B. Pan, S. B. Hait, K. Viswanathan and S. Joensson, *J. Polym. Sci., Part A: Polym. Chem.*, 2004, **42**, 4009-4015.
28. A. F. Senyurt and C. E. Hoyle, *Eur. Polym. J.*, 2006, **42**, 3133-3139.
29. A. Erddalane, J. P. Fouassier, F. Morlet-Savary and Y. Takimoto, *J. Polym. Sci., Part A: Polym. Chem.*, 1996, **34**, 633-642.
30. J. He and E. Wang, *Chin. J. Polym. Sci.*, 1990, **8**, 44-50.

31. D. Kim and J. W. Stansbury, *J. Polym. Sci., Part A: Polym. Chem.*, 2009, **47**, 3131-3141.
32. D. Kim, A. B. Scranton and J. W. Stansbury, *J. Appl. Polym. Sci.*, 2009, **114**, 1535-1542.
33. D. Kim and J. W. Stansbury, *J. Polym. Sci., Part A: Polym. Chem.*, 2009, **47**, 887-898.
34. C. Grotzinger, D. Burget, P. Jacques and J. P. Fouassier, *Polymer*, 2003, **44**, 3671-3677.
35. J. P. Fouassier, F. Morlet-Savary, K. Yamashita and S. Imahashi, *Polymer*, 1997, **38**, 1415-1421.
36. J. Kabatc, M. Zasada and J. Paczkowski, *J. Polym. Sci., Part A: Polym. Chem.*, 2007, **45**, 3626-3636.
37. J. Kabatc and J. Paczkowski, *J. Photochem. Photobiol. A: Chem.*, 2006, **184**, 184-192.
38. J. P. Fouassier, X. Allonas, J. Lalevee and M. Visconti, *J. Polym. Sci., Part A: Polym. Chem.*, 2000, **38**, 4531-4541.
39. J. P. Fouassier, D. Ruhlmann, B. Graff, Y. Takimoto, M. Kawabata and M. Harada, *J. Imaging Sci. Technol.*, 1993, **37**, 208-210.
40. O. I. Tarzi, X. Allonas, C. Ley and J.-P. Fouassier, *Journal of Polymer Science, Part A: Polymer Chemistry*, 2010, **48**, 2594-2603.
41. W. D. Cook and F. Chen, *J. Polym. Sci., Part A: Polym. Chem.*, 2011, **49** 5030-5041.
42. Y. Bi and D. C. Neckers, *Macromolecules*, 1994, **27**, 3683-3893.
43. Y. Yagci and Y. Hepuzer, *Macromolecules*, 1999, **32**, 6367-6370.
44. J. V. Crivello, *J. Macromol. Sci., Pure Appl. Chem.*, 2009, **46**, 474-483.
45. J. V. Crivello, *J. Polym. Sci., Part A: Polym. Chem.*, 2009, **47**, 866-875.
46. J. D. Oxman, D. W. Jacobs, M. C. Trom, V. Sipani, B. Ficek and A. B. Scranton, *J. Polym. Sci., Part A: Polym. Chem.*, 2005, **43**, 1747-1756.
47. J. V. Crivello and K. Dietliker, *Photoinitiators for free radical cationic and anionic photopolymerization*, Wiley, New York, 1988.
48. N. Arsu and M. Aydin, *Journal of Photochemistry and Photobiology A: Chemistry*, 1999, **127**, 143-145.
49. K. Dean and W. D. Cook, *Macromolecules*, 2002, **35**, 7942-7954.
50. W. D. Cook, *J. Polym. Sci., Part A: Polym. Chem.*, 1993, **31**, 1053-1067.
51. S. Chen, W. D. Cook and F. Chen, *Macromolecules*, 2009, **42**, 5965–5975.
52. W. D. Cook, S. Chen, F. Chen, M. U. Kahveci and Y. Yagci, *J. Polym. Sci., Part A: Polym. Chem.*, 2009, **47**, 5474–5487.
53. W. D. Cook, *J. Appl. Polym. Sci.*, 1991, **42**, 2209-2222.
54. T. F. Scott, W. D. Cook and J. S. Forsythe, *Polymer*, 2002, **43**, 5839-5845.
55. L. K. J. Tong and W. O. Kenyon, *J. Am. Chem. Soc.*, 1945, **67**, 1278-1281.
56. W. D. Cook, *Polymer*, 1992, **33**, 2152-2161.
57. G. Wisanrakkit and J. K. Gillham, *J. Appl. Polym. Sci.*, 1990, **41**, 2885-2929.
58. M. T. Aronhime and J. K. Gillham, *Adv. Polym. Sci.*, 1986, **78**, 83-113.
59. G. P. Simon, P. E. M. Allen and D. R. G. Williams, *Polymer*, 1991, **32**, 2577-2587.
60. F. Chen and W. D. Cook, *Eur. Polym. J.*, 2008, **44**, 1796-1813.
61. K. M. Dean and W. D. Cook, *Polym. Int.*, 2004, **53**, 1305-1313.
62. R. W. Yip, R. O. Loutfy, Y. L. Chow and L. K. Magdzinski, *Canadian Journal of Chemistry*, 1972, **50**, 3426-3431.
63. J. B. Guttenplan and S. G. Cohen, *Journal of the American Chemical Society*, 1972, **94**, 4040-4042.
64. R. D. Levin and S. G. Lias, *National Bureau of Standards, National Standard Reference Data Series*, 1982, **n 71**, 1971-1981.
65. D. Rehm and A. Weller, *Ber. Bunsenges. Phys. Chem.*, 1969, **73**, 834-839.
66. D. Rehm and A. Weller, *Isr. J. Chem.*, 1970, **8**, 259-271.
67. K. S. Padon, D. Kim, M. El-Maazawi and A. B. Scranton, *ACS Symp. Ser.*, 2003, **847**, 15-26.
68. H. J. Hageman, *Prog. Org. Coat.*, 1985, **13**, 123-150.
69. H. Block, A. Ledwith and A. R. Taylor, *Polymer*, 1971, **12**, 271-288.
70. V. Sipani, A. Kirsch and A. B. Scranton, *J. Polym. Sci., Part A: Polym. Chem.*, 2004, **42**, 4409-4416.

71. J. P. Fouassier, D. Burr and J. V. Crivello, *J. Photochem. Photobiol. A: Chem.*, 1989, **49**, 317-324.
72. G. Manivannan and J. P. Fouassier, *Journal of Polymer Science, Part A: Polymer Chemistry*, 1991, **29**, 1113-1124.
73. M. R. Rodrigues and M. G. Neumann, *Macromolecular Chemistry and Physics*, 2001, **202**, 2776-2782.
74. J. V. Crivello, *J. Polym. Sci., Part A: Polym. Chem.*, 1999, **37**, 4241-4254.
75. E. W. Nelson, T. P. Carter and A. B. Scranton, *J. Polym. Sci., Part A: Polym. Chem.*, 1995, **33**, 247-256.
76. Y. Hua and J. V. Crivello, *Macromolecules*, 2001, **34**, 2488-2494.
77. J. V. Crivello, J. M, F. Jiang, H. Hua, J. Ahn and R. Acosta Ortiz, *Macromol Symp*, 2004, **215**, 165-177.
78. Y. Bi and D. C. Neckers, *Journal of Photochemistry and Photobiology A: Chemistry*, 1993, **74**, 221-230.
79. S. W. Benson, *The foundations of chemical kinetics*, McGraw-Hill,, New York, 1960.
80. Y. Yagci, A. C. Aydogan and A. E. Sizgek, *J. Polym. Sci. Polym. Lett. Ed.*, 1984, **22**, 103-106.
81. M. Aydin, N. Arsu and Y. Yagci, *Macromol. Rapid Commun.*, 2003, **24**, 718–723.
82. C. Dworak and R. Liska, *Journal of Polymer Science, Part A: Polymer Chemistry* 2010, **48**, 5865-5871.
83. J. P. Fouassier, D. Burr and J. V. Crivello, *J. Macromol. Sci., Pure Appl. Chem.*, 1994, **A31**, 677-701.
84. Q. Q. Zhu, W. Schnabel and P. Jacques, *J. Chem. Soc., Faraday Trans.*, 1991, **87**, 1531-1535.
85. Y. Pan, W. Tang, T. Yu, J. Wang, Y. Fu, G. Wang and S. Yu, *J. Lumin.*, 2007, **126**, 421-426.
86. S. N. Sharma, H. Sharma, G. Singh and S. M. Shivaprasad, *Materials Chemistry and Physics*, 2008, **110**, 471-480.
87. M. L. Gomez, H. A. Montejano and C. M. Previtali, *Journal of Photochemistry and Photobiology A: Chemistry*, 2008, **197**, 18-24.

Graphical Table of Contents

Enhanced visible radiation photopolymerization of dimethacrylates with the three component thioxanthone (CPTXO) - amine - iodonium salt system.

Wayne D. Cook and Fei Chen

The three component thioxanthone/iodonium/amine visible light photoinitiator system is four times more efficient due to irreversible oxidation of the ketyl and the amine radicals by the iodonium salt and the regeneration of the thioxanthone and produce twice as many active radicals.